


## Composite topological phases via Floquet engineering

Hong Wu <sup>\*</sup>*School of Science, and Institute for Advanced Sciences, Chongqing University of Posts and Telecommunications, Chongqing 400065, China*

(Received 7 August 2023; accepted 30 October 2023; published 13 November 2023)

The hybridization of different topological phases is attractive because it can facilitate the simultaneous utilization of their respective advantages. Three-dimensional (3D) higher-order topological insulators host gapless hinge states or corner states, while Weyl semimetals have novel properties such as chiral anomaly. However, so far, the general method to induce 3D composite topological phases with coexisting Weyl semimetals and higher-order topological insulators is still lacking. Here, we propose a scheme to induce this kind of composite topological phase by periodic driving and demonstrate that such a phase is the intermediate phase between anomalous Floquet higher-order topological insulators and Floquet first-order Weyl semimetals. Our results may open a possibility to realize different phases without static analogs.

DOI: [10.1103/PhysRevB.108.195125](https://doi.org/10.1103/PhysRevB.108.195125)

### I. INTRODUCTION

Recently, traditional topological phases with gapless edge states [1–3] or surface Fermi arcs [4–10] have been extended to  $n$ th-order topological phases, which feature the presence of  $(d - n)$ -dimensional boundary states [11–29]. Both various theoretical schemes to realize these new phases [30–56] and some experimental observations [57–61] have been reported over the past few years. Explorations of physical systems supporting exotic topological states is a main theme of condensed matter physics. One of the interesting questions is whether different topological phases can coexist in one system. The proposal of this novel state has the following two meanings: (1) It can greatly enrich the family of topological states. (2) Various hybrid topological phases can take advantage of two kinds of different phases and be used to design bifunctional devices [62]. Although composite topological semimetals with nodal points and nodal lines [63], hybrid topological photonic crystals that can host simultaneously quantum anomalous Hall and valley Hall phases in different band gaps [64], and hybrid order topological insulators [65] have been found in several systems, the topological phases in all band gaps are either topological insulators or topological semimetals. A natural question is whether composite topological phases with topological semimetals and insulators can exist in a single system. Due to the different definitions of each topological phase, it seems to be difficult to achieve composite topological phases with several different topologies in a single system.

Coherent control via periodic driving dubbed Floquet engineering has become a versatile tool in artificially creating novel topological phases in systems of ultracold atoms [66,67], photonics [68,69], superconductor qubits [70], and graphene [71]. Inspired by the fact that periodic driving can generate new topological phases without static

analogues [65,72–77], whether the composite topological phases with coexisting Weyl semimetals and higher-order topological insulators can be induced by periodic driving is worth studying.

In this paper, we propose a scheme to artificially create three-dimensional (3D) composite topological phases with coexisting Weyl semimetals and higher-order topological insulators by Floquet engineering. The basic picture is illustrated in Fig. 1. Starting from a 3D anomalous Floquet higher-order topological insulator with gapless hinge states in both 0 and  $\pi/T$  gaps, we observe that the chiral hinge state in the  $\phi/T$  ( $\phi = 0$  or  $\pi$ ) gap can be destroyed by appropriate perturbations, and then the phase with high-order topology in this gap is converted to a Weyl semimetal. In the process of gradually increasing perturbation, the higher-order topological states in the  $\pi/T$  gap will be converted successively into second- and first-order Weyl semimetals, while the higher-order topological insulator in the 0 gap is maintained. A composite topological phase with a coexistence of a first- (second-) order Weyl semimetal and a higher topological order insulator will appear. When the perturbation is large enough, the phases in both gaps will become a Floquet first-order Weyl semimetal phase. Such a strategy that only takes advantage of two energy gaps in a periodically driven system can be used to induce various other composite topological phases.

### II. ANOMALOUS FLOQUET HIGHER-ORDER TOPOLOGICAL INSULATOR

We consider a static four-band model on a cubic lattice. Its Bloch Hamiltonian is

$$\begin{aligned} \mathcal{H}(\mathbf{k}) = & (v + \lambda \cos k_x)\tau_x\sigma_0 - (\lambda \sin k_x)\tau_y\sigma_z \\ & + (v + \lambda \cos k_y)\tau_y\sigma_y + (\lambda \sin k_y)\tau_x\sigma_x \\ & + \chi \cos k_z(\tau_x\sigma_0 + \tau_y\sigma_y) + \sqrt{2}\chi' \sin k_z\tau_z\sigma_0, \quad (1) \end{aligned}$$

<sup>\*</sup>wuh@cqupt.edu.cn

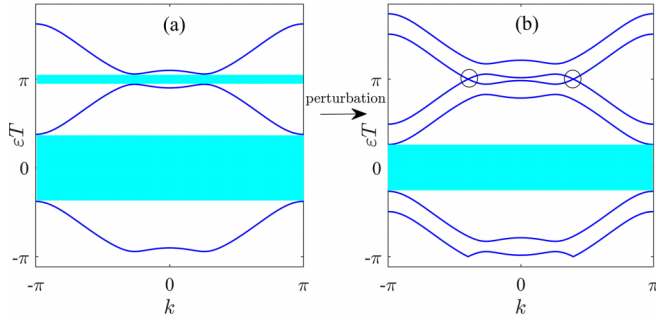


FIG. 1. Schematic of (a) an anomalous Floquet higher-order topological insulator and (b) a composite topological phase. As shown in (a), the band gap labeled in cyan color indicates that there are gapless chiral hinge states in this gap. According to topological classification, the higher-order topological number can be defined. So we believe that there is a higher-order topological phase at this gap. With the introduction of perturbation, two three-dimensional bands with a linear dispersion are degenerate at two isolated momentum points, which are called Weyl points. The existence of Weyl points indicates the formation of a Weyl semimetal phase at the  $\pi/T$  gap. Due to the topological charge of the Weyl point, Weyl semimetals can be sliced into a family of two-dimensional (2D) Chern and normal insulators parametrized by  $k_z$ . So we realize a second-order topological insulator in the quasienergy-0 gap, and a Weyl semimetal in the quasienergy- $\pi/T$  gap. Here, the dispersion relation is calculated using the parameters in Fig. 4(b).

where  $\sigma_i$  and  $\tau_i$  ( $i = x, y, z$ ) are the Pauli matrices acting on the spin and orbital degrees of freedom, respectively.  $\tau_0$  and  $\sigma_0$  are identity matrices. The system has mirror-rotation symmetry  $\mathcal{M}_{xy}\mathcal{H}(k_x, k_y, k_z)\mathcal{M}_{xy}^{-1} = \mathcal{H}(k_y, k_x, k_z)$  with  $\mathcal{M}_{xy} = [(\tau_0 - \tau_z)\sigma_x - (\tau_0 + \tau_z)\sigma_z]/2$ . Along the high-symmetry line  $k_x = k_y = k$ ,  $\mathcal{H}(\mathbf{k})$  can be expressed as  $\text{diag}[\mathcal{H}_+(k, k_z), \mathcal{H}_-(k, k_z)]$  with  $\mathcal{H}_\pm(k, k_z) = \mathbf{h}_\pm \cdot \boldsymbol{\sigma}$  and  $\mathbf{h}_\pm = \sqrt{2}[(\chi \cos k_z + v + \lambda \cos k), \pm(\lambda \sin k), \chi' \sin k_z]$ . Its topology is described by the mirror Chern number  $\mathcal{C} = (\mathcal{C}_+ - \mathcal{C}_-)/2$  with  $\mathcal{C}_\pm = \frac{1}{4\pi} \int_{\text{BZ}} \frac{1}{E^{3/2}} \mathbf{h}_\pm \cdot (\partial_k \mathbf{h}_\pm \times \partial_{k_z} \mathbf{h}_\pm) d^2\mathbf{k}$  [78,79]. For our system, the Chern number  $\mathcal{C}$  can be  $\pm 1$  and 0. When  $\mathcal{C}$  is nonzero, there are four gapless chiral hinge states in the bulk gap. The underlying mechanism for the formation of hinge states can be explained by surface theory. For our higher-order topological phase, the mass terms of adjacent side surfaces have opposite sign [78], so the hinge is a domain wall of the Dirac mass and consequently harbors a hinge state. A higher-order topological insulator with mirror-rotation symmetry is also studied in Ref. [78]. We consider the periodically driven scenario as

$$\lambda(t) = \begin{cases} \lambda_1, & t \in [NT, NT + T_1), \\ \lambda_2, & t \in [NT + T_1, (N + 1)T), \end{cases} \quad (2)$$

where  $T$  ( $T = T_1 + T_2$ ) is the driving period. Due to the fact that the energy of our system is not conserved, this kind of time-periodic system does not have a well-defined energy spectrum. According to the Floquet theorem, the one-period evolution operator  $U(T) = \mathbb{T} e^{-i \int_0^T \mathcal{H}(t) dt}$  defines an effective Hamiltonian  $\mathcal{H}_{\text{eff}} \equiv \frac{i}{T} \ln U(T)$  whose eigenvalues are called quasienergies [80]. From the eigenvalue equation  $U(T)|u_i\rangle =$

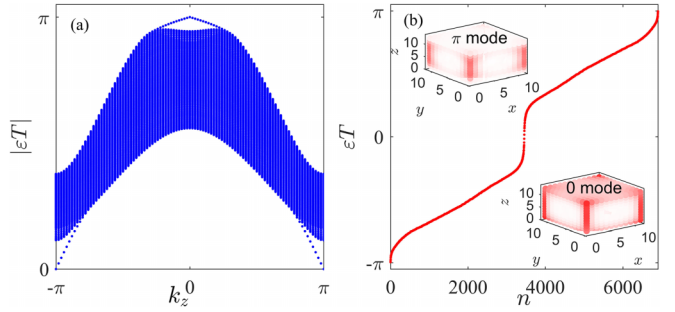


FIG. 2. Quasienergy spectrum under the  $x, y$  direction open boundary condition in (a) and the  $x, y, z$  direction open boundary condition in (b). The insets of (b) show the probability distribution of the 0 mode and  $\pi/T$  mode hinge states, respectively. We use  $v = 1.3$ ,  $\lambda_1 = -\lambda_2 = 1.5$ ,  $\chi = \chi' = 1$ ,  $T_1 = 0.2$ , and  $T_2 = 0.6$ .

$e^{-i\varepsilon_i T}|u_i\rangle$ , we conclude that the quasienergy is a phase factor, which is defined modulus  $2\pi/T$  and takes values in the first quasienergy Brillouin zone  $[-\pi/T, \pi/T]$  [81]. The topological phases of our periodically driven system are defined in such a quasienergy spectrum. Correspondingly, edge modes can occur at both the quasienergies 0 and  $\pi/T$  [82]. It means that two topological invariants which separately count the edge modes at 0 and  $\pi/T$  are needed. Inspired by the definition of a topological invariant in a static second-order topological insulator and the unique topology in periodically driven systems [78,83,84], we can construct a pair of topological indices  $\mathcal{V}_\phi$  ( $\phi$  is 0 or  $\pi$ ) that is equal to the number of the gapless hinge states at the  $\phi/T$  quasienergy. Along the high-symmetry line  $k_x = k_y = k$ ,  $U(k, k, k_z, t)$  can be diagonalized into  $\text{diag}[U_+(k, k_z, t), U_-(k, k_z, t)]$ . The dynamical winding number which characterizes the number of gapless hinge states at  $\phi/T$  ( $\phi = 0$  or  $\pi$ ) quasienergy is  $\mathcal{V}_\phi = \mathcal{V}_{\phi,+} - \mathcal{V}_{\phi,-}$  with

$$\mathcal{V}_{\phi,\pm} = \frac{1}{24\pi^2} \int_0^T dt \int dk dk_z \varepsilon^{i_1 i_2 i_3} \times \text{Tr}[U_{\phi,\pm}^\dagger \partial_{i_1} U_{\phi,\pm} U_{\phi,\pm}^\dagger \partial_{i_2} U_{\phi,\pm} U_{\phi,\pm}^\dagger \partial_{i_3} U_{\phi,\pm}], \quad (3)$$

where  $U_{\phi,\pm} = U_\pm(k, k_z, t)[U_\pm(k, k_z, T)]_\phi^{-t/T}$  with

$$[U_\pm(k, k_z, T)]_\phi^{-t/T} = \sum_l \exp\left[-\frac{t}{T} \log_\phi e^{-i\varepsilon_{\mathbf{k},l,\pm} T}\right] P_{l,\pm}(\mathbf{k}, T). \quad (4)$$

Here,  $\varepsilon_{\mathbf{k},l,\pm} T$  labels the quasienergy bands derived from  $U_\pm(\mathbf{k}, T)$  satisfying  $\varepsilon_{\mathbf{k},l,\pm} T \in [\phi, \phi + 2\pi)$  and  $P_{l,\pm}(\mathbf{k}, T)$  is the projection matrix given by the eigenvector of  $\varepsilon_{\mathbf{k},l,\pm} T$  [78,83,84]. The relationship between  $\mathcal{V}_\phi$  and Chern number  $\mathcal{C}$  is  $\mathcal{V}_\pi - \mathcal{V}_0 = \mathcal{C}$ . Figure 2(a) shows the anomalous Floquet higher-order topological insulator which hosts robust gapless chiral hinge modes even when its bulk Floquet bands carry trivial mirror Chern numbers  $\mathcal{C} = \mathcal{V}_\pi - \mathcal{V}_0 = 1 - 1 = 0$  [85]. The corresponding quasienergy spectrum under an open boundary condition along three directions in Fig. 2(b) has gapless chiral hinge states at quasienergies 0 and  $\pi/T$  [see the inset of Fig. 2(b)]. It signifies the formation of a 3D second-order topological insulator. On this basis, we will

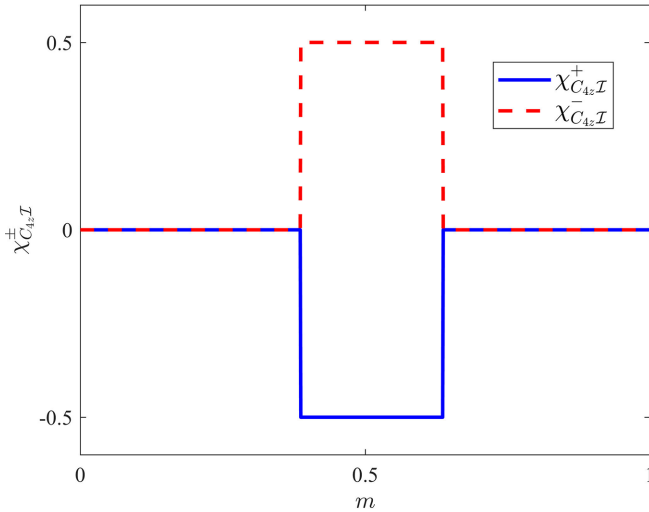


FIG. 3. The  $\chi_{C_{4z}\mathcal{I}}^{\pm}$  as the change of  $m$ . The other parameters are the same as in Fig. 2.

further discuss the formation mechanism of composite topological phases in the following sections.

### III. METHOD TO OBTAIN COMPOSITE TOPOLOGICAL PHASES

By applying appropriate perturbation to our anomalous Floquet higher-order topological insulator shown in Fig. 2, a phase with higher-order topology in the  $\pi/T$  gap can be converted to Weyl semimetals and we can realize composite topological phases with coexisting Weyl semimetals and second-order topological insulators. We consider  $\mathcal{H}' = \mathcal{H} + m\tau_0\sigma_y$ , which breaks mirror-rotation symmetry, but preserves rotoinversion symmetry  $C_{4z}\mathcal{I}$ . The operator  $C_{4z}\mathcal{I}$  changes wave vectors as  $(k_x, k_y, k_z) \rightarrow (k_y, -k_x, -k_z)$ . Four  $C_{4z}\mathcal{I}$  invariant points in the  $\mathbf{k}$  space are  $K_4 = \{\Gamma = (0, 0, 0), M = (\pi, \pi, 0), Z = (0, 0, \pi), A = (\pi, \pi, \pi)\}$ . The topological indices which describe the higher-order topology in rotoinversion-symmetric system are

$$\begin{aligned} \chi_{C_{4z}\mathcal{I}}^{\pm} = & \frac{1}{2} [n_{\pm\frac{\pi}{4}}(Z) - n_{\mp\frac{3\pi}{4}}(Z) + n_{\pm\frac{\pi}{4}}(A) \\ & - n_{\mp\frac{3\pi}{4}}(A) - n_{\pm\frac{\pi}{4}}(\Gamma) + n_{\mp\frac{3\pi}{4}}(\Gamma) \\ & - n_{\pm\frac{\pi}{4}}(M) + n_{\mp\frac{3\pi}{4}}(M)] \bmod 2, \end{aligned} \quad (5)$$

where  $n_{+\frac{\pi}{4}}(\mathbf{k})$ ,  $n_{-\frac{\pi}{4}}(\mathbf{k})$ ,  $n_{+\frac{3\pi}{4}}(\mathbf{k})$ , and  $n_{-\frac{3\pi}{4}}(\mathbf{k})$  are the numbers of occupied states with  $C_{4z}\mathcal{I}$  eigenvalues,  $e^{i\frac{\pi}{4}}$ ,  $e^{-i\frac{\pi}{4}}$ ,  $e^{i\frac{3\pi}{4}}$ , and  $e^{-i\frac{3\pi}{4}}$  at  $\mathbf{k}$ , respectively [86]. When  $\chi_{C_{4z}\mathcal{I}}^{\pm}$  are both nonzero, chiral hinge modes appear in the static system. The effective Hamiltonian  $\mathcal{H}'_{\text{eff}}$  inherits the rotoinversion symmetry, which suffices to study the system via topological indices in Eq. (5). Due to the fact that  $\chi_{C_{4z}\mathcal{I}}^{\pm}$  are  $Z_2$  indices, the topological indices of previous anomalous Floquet higher-order topological insulators are zero [87]. Once the higher-order topology in the  $\pi/T$  gap is destroyed, the topological indices will be nontrivial. They may just be used to describe the higher-order topology of our composite topological states.

Figure 3 shows the topological indices with the change of the perturbation strength.  $\chi_{C_{4z}\mathcal{I}}^{\pm}$  for anomalous Floquet higher-

order topological insulators at  $m = 0$  are 0. The two phase transition points  $m = 0.3864$  and  $m = 0.6364$  correspond to the position where the  $\pi/T$  mode and 0 mode hinge states disappear, respectively. When  $0.3864 < m < 0.6364$ , the phase with higher-order topology in the  $\pi/T$  gap has been converted to a Weyl semimetal phase (see the next section for details).  $\chi_{C_{4z}\mathcal{I}}^{\pm} = \pm 0.5$  for such composite topological states is nontrivial.

### IV. TWO KINDS OF COMPOSITE TOPOLOGICAL PHASES

To reveal the detailed process of inducing composite topological states, we plot in Fig. 4 the quasienergy spectra for different perturbation  $m$  and corresponding  $k_z$ -dependent Chern numbers.  $\mathcal{C}(k_z)$  is defined as

$$\mathcal{C}(k_z) = \frac{1}{2\pi} \int_0^{2\pi} dk_x \int_0^{2\pi} dk_y [\partial_{k_x} A_{k_y} - \partial_{k_y} A_{k_x}], \quad (6)$$

where  $A_{k_{x,y}} = i\langle \psi(k_x, k_y, k_z) | \partial_{k_{x,y}} | \psi(k_x, k_y, k_z) \rangle$  with  $|\psi(k_x, k_y, k_z)\rangle$  being the eigenstate of  $\mathcal{H}'_{\text{eff}}$  [88]. Based on the quasienergy spectrum in Fig. 4(a) and the corresponding Chern number in Fig. 4(d), we can know that there are two pairs of Weyl points (black dots A, B, C, D) at quasienergy  $\pi/T$ . The existence of Weyl points indicates the formation of a Weyl semimetal phase. Furthermore, the gapless chiral hinge states demonstrate the higher-order topology in the  $\pi/T$  gap. These results confirm the higher-order Weyl semimetal phase which is similar to the one studied in Ref. [86]. Unlike the higher-order Weyl semimetals in the  $\pi/T$  gap, the gapped bulk band and gapless chiral hinge states at the 0 gap show a higher-order topological insulator phase. Therefore, an interesting phase with the coexistence of higher-order Weyl semimetals and higher-order topological insulators has been induced. In fact, this is an intermediate state from an anomalous Floquet higher-order topological insulator to another composite topological state. With the increase of  $m$ , Weyl points B and C will meet at  $k_z = 0$ , resulting in the disappearance of the hinge state in the  $\pi/T$  gap. The higher-order Weyl semimetal phase in the  $\pi/T$  gap will be converted to traditional first-order Weyl semimetal phases. It is seen from Fig. 4(e) that the 3D phase in the  $\pi/T$  gap shown in Fig. 4(b) can be sliced into a family of two-dimensional (2D) Chern topological insulators ( $|k_z| < 1.194$ ) and normal insulators ( $|k_z| > 1.194$ ) parametrized by  $k_z$ . Two Weyl points are present where  $\mathcal{C}(k_z)$  jumps between 0 and  $-1$ . It is remarkable to find that the phase with higher-order topology in the  $\pi/T$  gap has been converted to a traditional Weyl semimetal phase. Such a coexistence of first-order Weyl semimetals and second-order topological insulators is absent in its original static Hamiltonian. When  $m$  is large enough, both the hinge states in the 0 gap and  $\pi/T$  gap will be destroyed [as shown in Fig. 4(c)]. According to the Chern number  $\mathcal{C}_0$  and  $\mathcal{C}_{\pi/T}$  in Fig. 4(f), the higher-order topological insulators in both the 0 gap and  $\pi/T$  gap have been converted to first-order Weyl semimetal phases. These results confirm the superiority of the periodic driving in synthesizing a different composite topological phase.

Based on Figs. 3 and 4, it is concluded that the transition from a phase with higher-order topology to traditional first-order Weyl semimetals is accompanied by the emergence of

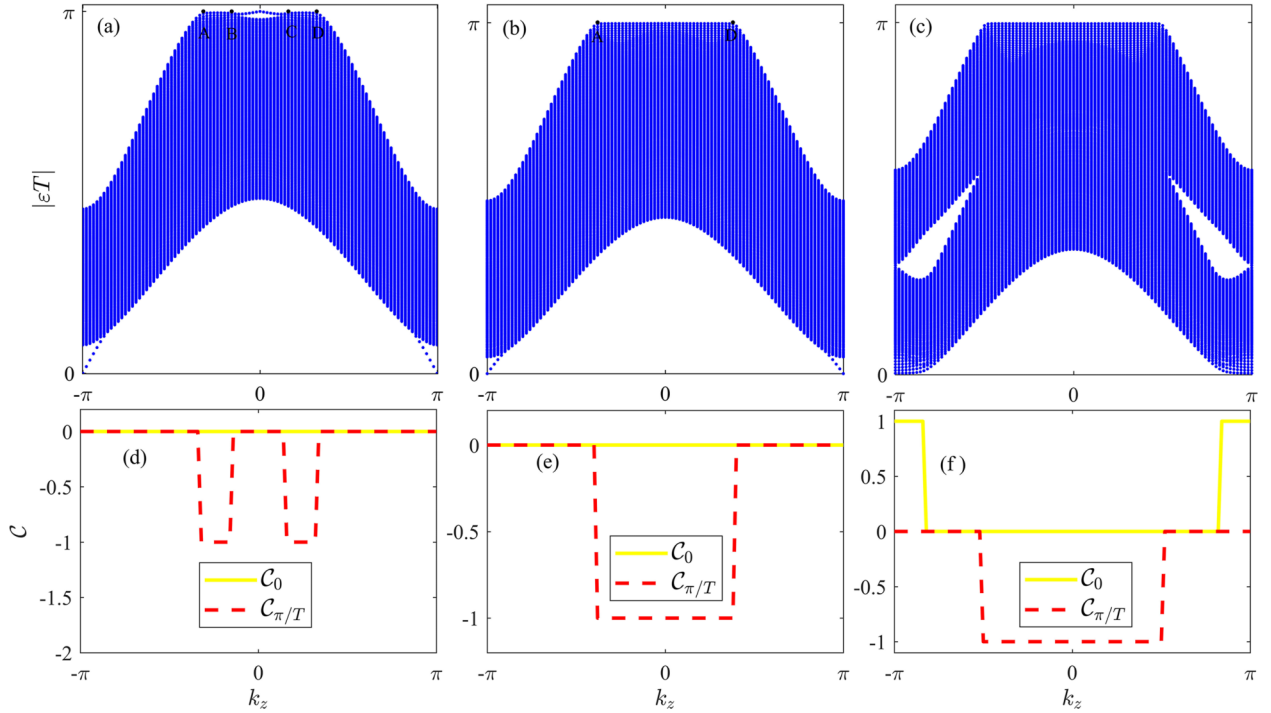


FIG. 4. Quasienergy spectrum under the  $x, y$  direction open boundary condition in (a)–(c) and the corresponding Chern numbers  $C_0$  (yellow solid) and  $C_{\pi/T}$  (red dashed) in (d)–(f) with the change of  $k_z$ . Here,  $C_{\pi/T}$  and  $C_0$  are calculated for the first and second band, respectively (according to the magnitude of energy, the four bands can be labeled as  $\varepsilon_1 T < \varepsilon_2 T < \varepsilon_3 T < \varepsilon_4 T$ ). We use  $m = 0.30$  in (a),  $0.45$  in (b), and  $0.8$  in (c). The other parameters are the same as in Fig. 2.

Weyl points at  $k_z = 0$  ( $k_z = \pi$ ) for  $m = 0.3864$  ( $m = 0.6364$ ), and the value of  $m$  at these two phase transition points can be obtained analytically. Considering  $k_z = 0$  or  $\pi$  and  $k_x = k_y = k = 0$  or  $\pi$ , which leads to  $[\mathcal{H}'(\lambda = \lambda_1), \mathcal{H}'(\lambda = \lambda_2)] = 0$ , the corresponding eigenvalues of the effective Hamiltonian are

$$\varepsilon T = \pm(T_1 + T_2)m \pm \sqrt{2}|(T_1 - T_2)\lambda \cos(k) + (T_1 + T_2)[v + \cos(k_z)]|, \quad (7)$$

where  $\lambda = \lambda_1 = -\lambda_2$ . The band touching points at  $m = 0.3864$  ( $\varepsilon T = \pi$ ) and  $m = 0.6364$  ( $\varepsilon T = 0$ ) can be obtained by setting  $k_z = 0, k = \pi$  and  $k_z = \pi, k = 0$ , respectively.

Although two kinds of composite topological phases have been observed in Fig. 4, the surface states of Weyl semimetals are not clearly shown. The existence of Weyl semimetals is manifested in the topological surface states which are called Fermi arcs. The entire quasienergy spectrum in Fig. 5 can show the existence of lines connecting Weyl points with opposite chiralities, which is analogous to the Fermi arc in static Weyl semimetal systems. These  $0$  or  $\pi/T$  mode edge states in Fig. 5 are directly related to the corresponding  $k_z$ -dependent Chern number in Fig. 4. When  $C_0(k_z)$  or  $C_{\pi/T}(k_z)$  is nonzero, the quasienergy spectrum of the 2D sliced system at fixed  $k_z$  will show gapless chiral edge states which originate from the topology of the Chern insulator. These gapless chiral edge states cross at  $k_y = 0$  or  $\pi$ . All edge state crossings are what appear as a Fermi arc joining two Weyl points [89,90]. All these results reconfirm the existence of Weyl semimetals.

## V. DISCUSSION AND CONCLUSION

The static second-order topological insulators have been observed in several systems [60,61,91–93], in the latter of which the static higher-order topological insulators of our 2D subsystems have been realized. Periodic driving has been used to generate different topological phases in systems of

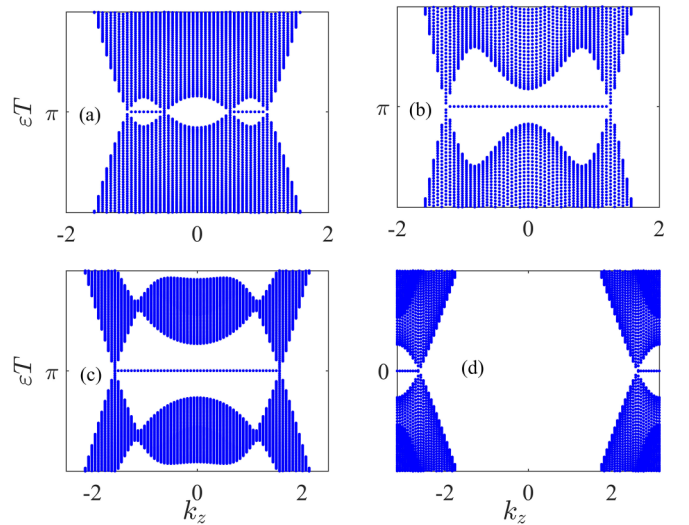


FIG. 5. Surface Fermi arcs connecting bulk nodes. We use  $m = 0.30, k_y = \pi$  in (a),  $m = 0.45, k_y = \pi$  in (b),  $m = 0.8, k_y = \pi$  in (c), and  $m = 0.8, k_y = 0$  in (d). The other parameters are the same as in Fig. 2.



ultracold atoms [66,67], photonics [68,69], superconductor qubits [70], graphene [71], and circuit [94]. We believe that our result may be realizable in the recent state-of-the-art experiment.

In summary, we have developed a method to induce a composite topological phase with the coexistence of Weyl semimetals and higher-order topological insulators by periodic driving. The corresponding complete description of such a phase is established. Such a strategy that only takes

advantage of two energy gaps in a periodically driven system can be used to induce various other hybrid topological phases.

#### ACKNOWLEDGMENT

We would like to acknowledge helpful discussions with Lu-Rao Liu, and the support by a startup grant at Chongqing University of Posts and Telecommunications.

- 
- [1] X.-L. Qi and S.-C. Zhang, *Rev. Mod. Phys.* **83**, 1057 (2011).
- [2] A. Bansil, H. Lin, and T. Das, *Rev. Mod. Phys.* **88**, 021004 (2016).
- [3] M. Z. Hasan and C. L. Kane, *Rev. Mod. Phys.* **82**, 3045 (2010).
- [4] N. P. Armitage, E. J. Mele, and A. Vishwanath, *Rev. Mod. Phys.* **90**, 015001 (2018).
- [5] B. Q. Lv, H. M. Weng, B. B. Fu, X. P. Wang, H. Miao, J. Ma, P. Richard, X. C. Huang, L. X. Zhao, G. F. Chen, Z. Fang, X. Dai, T. Qian, and H. Ding, *Phys. Rev. X* **5**, 031013 (2015).
- [6] C. Fang, M. J. Gilbert, X. Dai, and B. A. Bernevig, *Phys. Rev. Lett.* **108**, 266802 (2012).
- [7] A. Lau, K. Koepf, J. van den Brink, and C. Ortix, *Phys. Rev. Lett.* **119**, 076801 (2017).
- [8] N. Xu, G. Autès, C. E. Matt, B. Q. Lv, M. Y. Yao, F. Bisti, V. N. Strocov, D. Gawryluk, E. Pomjakushina, K. Conder, N. C. Plumb, M. Radovic, T. Qian, O. V. Yazyev, J. Mesot, H. Ding, and M. Shi, *Phys. Rev. Lett.* **118**, 106406 (2017).
- [9] J. Schusser, H. Bentmann, M. Ünzelmann, T. Figgemeier, C.-H. Min, S. Moser, J. N. Neu, T. Siegrist, and F. Reinert, *Phys. Rev. Lett.* **129**, 246404 (2022).
- [10] Tena Dubček, C. J. Kennedy, L. Lu, W. Ketterle, M. Soljačić, and H. Buljan, *Phys. Rev. Lett.* **114**, 225301 (2015).
- [11] W. A. Benalcazar, B. A. Bernevig, and T. L. Hughes, *Science* **357**, 61 (2017).
- [12] F. Schindler, A. M. Cook, M. G. Vergniory, Z. Wang, S. S. P. Parkin, B. A. Bernevig, and T. Neupert, *Sci. Adv.* **4**, eaat0346 (2018).
- [13] L. Trifunovic and P. W. Brouwer, *Phys. Rev. X* **9**, 011012 (2019).
- [14] F. Liu and K. Wakabayashi, *Phys. Rev. Lett.* **118**, 076803 (2017).
- [15] Z. Song, Z. Fang, and C. Fang, *Phys. Rev. Lett.* **119**, 246402 (2017).
- [16] J.-H. Wang, Y.-B. Yang, N. Dai, and Y. Xu, *Phys. Rev. Lett.* **126**, 206404 (2021).
- [17] S. A. A. Ghorashi, T. Li, and T. L. Hughes, *Phys. Rev. Lett.* **125**, 266804 (2020).
- [18] H.-X. Wang, Z.-K. Lin, B. Jiang, G.-Y. Guo, and J.-H. Jiang, *Phys. Rev. Lett.* **125**, 146401 (2020).
- [19] Z.-Q. Zhang, B.-L. Wu, C.-Z. Chen, and H. Jiang, *Phys. Rev. B* **104**, 014203 (2021).
- [20] S. Ghosh, K. Saha, and K. Sengupta, *Phys. Rev. B* **105**, 224312 (2022).
- [21] X.-L. Du, R. Chen, R. Wang, and D.-H. Xu, *Phys. Rev. B* **105**, L081102 (2022).
- [22] Z. Wang, D. Liu, H. T. Teo, Q. Wang, H. Xue, and B. Zhang, *Phys. Rev. B* **105**, L060101 (2022).
- [23] Q. Wei, X. Zhang, W. Deng, J. Lu, X. Huang, M. Yan, G. Chen, Z. Liu, and S. Jia, *Nat. Mater.* **20**, 812 (2021).
- [24] C. Chen, X.-T. Zeng, Z. Chen, Y. X. Zhao, X.-L. Sheng, and S. A. Yang, *Phys. Rev. Lett.* **128**, 026405 (2022).
- [25] S. Simon, M. Geier, and P. W. Brouwer, *Phys. Rev. B* **106**, 035105 (2022).
- [26] W. Zhu, M. Umer, and J. Gong, *Phys. Rev. Res.* **3**, L032026 (2021).
- [27] T. Liu, J. J. He, Z. Yang, and F. Nori, *Phys. Rev. Lett.* **127**, 196801 (2021).
- [28] Y. Zhou and P. Ye, *Phys. Rev. B* **107**, 085108 (2023).
- [29] Y.-F. Mao, Y.-L. Tao, J.-H. Wang, Q.-B. Zeng, and Y. Xu, *arXiv:2307.14974*.
- [30] M. Ezawa, *Phys. Rev. Lett.* **120**, 026801 (2018).
- [31] Y. Wang, Y. Ke, Y.-J. Chang, Y.-H. Lu, J. Gao, C. Lee, and X.-M. Jin, *Phys. Rev. B* **104**, 224303 (2021).
- [32] Y. Fang and J. Cano, *Phys. Rev. B* **101**, 245110 (2020).
- [33] H. Liu, S. Franca, A. G. Moghaddam, F. Hassler, and I. C. Fulga, *Phys. Rev. B* **103**, 115428 (2021).
- [34] Y. Otaki and T. Fukui, *Phys. Rev. B* **100**, 245108 (2019).
- [35] H. Li and K. Sun, *Phys. Rev. Lett.* **124**, 036401 (2020).
- [36] Z. Yan, *Phys. Rev. Lett.* **123**, 177001 (2019).
- [37] R. Queiroz and A. Stern, *Phys. Rev. Lett.* **123**, 036802 (2019).
- [38] A. Matsugatani and H. Watanabe, *Phys. Rev. B* **98**, 205129 (2018).
- [39] W. A. Benalcazar and A. Cerjan, *Phys. Rev. Lett.* **128**, 127601 (2022).
- [40] A. K. Ghosh, G. C. Paul, and A. Saha, *Phys. Rev. B* **101**, 235403 (2020).
- [41] Y. Han and A.-L. He, *Phys. Rev. B* **104**, 165416 (2021).
- [42] Y. Chen, F. Meng, Y. Kivshar, B. Jia, and X. Huang, *Phys. Rev. Res.* **2**, 023115 (2020).
- [43] M. J. Park, Y. Kim, G. Y. Cho, and S. B. Lee, *Phys. Rev. Lett.* **123**, 216803 (2019).
- [44] Y. Xue, H. Huan, B. Zhao, Y. Luo, Z. Zhang, and Z. Yang, *Phys. Rev. Res.* **3**, L042044 (2021).
- [45] E. Khalaf, *Phys. Rev. B* **97**, 205136 (2018).
- [46] B. Wang, X. Zhou, H. Lin, and A. Bansil, *Phys. Rev. B* **104**, L121108 (2021).
- [47] T. Mizoguchi, Y. Kuno, and Y. Hatsugai, *Phys. Rev. Lett.* **126**, 016802 (2021).
- [48] Y.-T. Hsu, W. S. Cole, R.-X. Zhang, and J. D. Sau, *Phys. Rev. Lett.* **125**, 097001 (2020).
- [49] M. Hirayama, R. Takahashi, S. Matsuishi, H. Hosono, and S. Murakami, *Phys. Rev. Res.* **2**, 043131 (2020).
- [50] C. Li, M. Li, L. Yan, S. Ye, X. Hu, Q. Gong, and Y. Li, *Phys. Rev. Res.* **4**, 023049 (2022).

- [51] O. Pozo, C. Repellin, and A. G. Grushin, *Phys. Rev. Lett.* **123**, 247401 (2019).
- [52] Y.-J. Wu, C.-C. Liu, and J. Hou, *Phys. Rev. A* **101**, 043833 (2020).
- [53] S. Qian, G.-B. Liu, C.-C. Liu, and Y. Yao, *Phys. Rev. B* **105**, 045417 (2022).
- [54] Z. Wu, Z. Yan, and W. Huang, *Phys. Rev. B* **99**, 020508(R) (2019).
- [55] S. Regmi, M. M. Hosen, B. Ghosh, B. Singh, G. Dhakal, C. Sims, B. Wang, F. Kabir, K. Dimitri, Y. Liu, A. Agarwal, H. Lin, D. Kaczorowski, A. Bansil, and M. Neupane, *Phys. Rev. B* **102**, 165153 (2020).
- [56] G. Salerno, G. Palumbo, N. Goldman, and M. Di Liberto, *Phys. Rev. Res.* **2**, 013348 (2020).
- [57] A. Cerjan, M. Jürgensen, W. A. Benalcazar, S. Mukherjee, and M. C. Rechtsman, *Phys. Rev. Lett.* **125**, 213901 (2020).
- [58] W. Zhang, D. Zou, Q. Pei, W. He, J. Bao, H. Sun, and X. Zhang, *Phys. Rev. Lett.* **126**, 146802 (2021).
- [59] H. Fan, B. Xia, L. Tong, S. Zheng, and D. Yu, *Phys. Rev. Lett.* **122**, 204301 (2019).
- [60] Z.-Z. Yang, X. Li, Y.-Y. Peng, X.-Y. Zou, and J.-C. Cheng, *Phys. Rev. Lett.* **125**, 255502 (2020).
- [61] B.-Y. Xie, G.-X. Su, H.-F. Wang, H. Su, X.-P. Shen, P. Zhan, M.-H. Lu, Z.-L. Wang, and Y.-F. Chen, *Phys. Rev. Lett.* **122**, 233903 (2019).
- [62] Y. Yang, J. Lu, M. Yan, X. Huang, W. Deng, and Z. Liu, *Phys. Rev. Lett.* **126**, 156801 (2021).
- [63] R. W. Bomantara, G. N. Raghava, L. Zhou, and J. Gong, *Phys. Rev. E* **93**, 022209 (2016).
- [64] Y. Wang, H.-X. Wang, L. Liang, W. Zhu, L. Fan, Z.-K. Lin, F. Li, X. Zhang, P.-G. Luan, Y. Poo, J.-H. Jiang, and G.-Y. Guo, *Nat. Commun.* **14**, 4457 (2023).
- [65] W. Zhu, Y. D. Chong, and J. Gong, *Phys. Rev. B* **103**, L041402 (2021).
- [66] A. Eckardt, *Rev. Mod. Phys.* **89**, 011004 (2017).
- [67] F. Meinert, M. J. Mark, K. Lauber, A. J. Daley, and H.-C. Nägerl, *Phys. Rev. Lett.* **116**, 205301 (2016).
- [68] M. C. Rechtsman, J. M. Zeuner, Y. Plotnik, Y. Lumer, D. Podolsky, F. Dreisow, S. Nolte, M. Segev, and A. Szameit, *Nature (London)* **496**, 196 (2013).
- [69] Q. Cheng, Y. Pan, H. Wang, C. Zhang, D. Yu, A. Gover, H. Zhang, T. Li, L. Zhou, and S. Zhu, *Phys. Rev. Lett.* **122**, 173901 (2019).
- [70] P. Roushan, C. Neill, A. Megrant, Y. Chen, R. Babbush, R. Barends, B. Campbell, Z. Chen, B. Chiaro, A. Dunsworth, A. Fowler, E. Jeffrey, J. Kelly, E. Lucero, J. Mutus, P. J. J. O'Malley, M. Neeley, C. Quintana, D. Sank, A. Vainsencher *et al.*, *Nat. Phys.* **13**, 146 (2017).
- [71] J. W. McIver, B. Schulte, F.-U. Stein, T. Matsuyama, G. Jotzu, G. Meier, and A. Cavalleri, *Nat. Phys.* **16**, 38 (2020).
- [72] H. Hu, B. Huang, E. Zhao, and W. V. Liu, *Phys. Rev. Lett.* **124**, 057001 (2020).
- [73] M. Rodriguez-Vega, A. Kumar, and B. Seradjeh, *Phys. Rev. B* **100**, 085138 (2019).
- [74] T. Nag, V. Juričić, and B. Roy, *Phys. Rev. Res.* **1**, 032045(R) (2019).
- [75] H. Wu and J.-H. An, *Phys. Rev. B* **107**, 235132 (2023).
- [76] H. Liu, T.-S. Xiong, W. Zhang, and J.-H. An, *Phys. Rev. A* **100**, 023622 (2019).
- [77] K. Yang, S. Xu, L. Zhou, Z. Zhao, T. Xie, Z. Ding, W. Ma, J. Gong, F. Shi, and J. Du, *Phys. Rev. B* **106**, 184106 (2022).
- [78] T. Liu, Y.-R. Zhang, Q. Ai, Z. Gong, K. Kawabata, M. Ueda, and F. Nori, *Phys. Rev. Lett.* **122**, 076801 (2019).
- [79] H. Wu, B.-Q. Wang, and J.-H. An, *Phys. Rev. B* **103**, L041115 (2021).
- [80] C. Chen, J.-H. An, H.-G. Luo, C. P. Sun, and C. H. Oh, *Phys. Rev. A* **91**, 052122 (2015).
- [81] A. Kundu, H. A. Fertig, and B. Seradjeh, *Phys. Rev. Lett.* **113**, 236803 (2014).
- [82] S. Yao, Z. Yan, and Z. Wang, *Phys. Rev. B* **96**, 195303 (2017).
- [83] M. S. Rudner, N. H. Lindner, E. Berg, and M. Levin, *Phys. Rev. X* **3**, 031005 (2013).
- [84] J. Yu, Y. Ge, and S. Das Sarma, *Phys. Rev. B* **104**, L180303 (2021).
- [85] R.-X. Zhang and Z.-C. Yang, [arXiv:2010.07945](https://arxiv.org/abs/2010.07945).
- [86] Y. Tanaka, R. Takahashi, R. Okugawa, and S. Murakami, *Phys. Rev. B* **105**, 115119 (2022).
- [87] A. A. Soluyanov and D. Vanderbilt, *Phys. Rev. B* **83**, 035108 (2011).
- [88] L.-J. Lang, X. Cai, and S. Chen, *Phys. Rev. Lett.* **108**, 220401 (2012).
- [89] Z.-M. Yu, W. Wu, Y. X. Zhao, and S. A. Yang, *Phys. Rev. B* **100**, 041118(R) (2019).
- [90] T. M. McCormick, I. Kimchi, and N. Trivedi, *Phys. Rev. B* **95**, 075133 (2017).
- [91] Q. Wei, X. Zhang, W. Deng, J. Lu, X. Huang, M. Yan, G. Chen, Z. Liu, and S. Jia, *Phys. Rev. Lett.* **127**, 255501 (2021).
- [92] M. Serra-Garcia, V. Peri, R. Süsstrunk, O. R. Bilal, T. Larsen, L. G. Villanueva, and S. D. Huber, *Nature (London)* **555**, 342 (2018).
- [93] S. Imhof, C. Berger, F. Bayer, J. Brehm, L. W. Molenkamp, T. Kiessling, F. Schindler, C. H. Lee, M. Greiter, T. Neupert, and R. Thomale, *Nat. Phys.* **14**, 925 (2018).
- [94] M. Chitsazi, H. Li, F. M. Ellis, and T. Kottos, *Phys. Rev. Lett.* **119**, 093901 (2017).